Range Identification for Perspective Dynamic Systems Using Linear Approximation

Lili Ma, *Student Member, IEEE*, YangQuan Chen† and Kevin L. Moore, *Senior Members, IEEE*
Center for Self-Organizing and Intelligent Systems (CSOIS),
Dept. of Electrical and Computer Engineering, 4160 Old Main Hill,
Utah State University (USU), Logan, UT 84322-4160, USA.
Email: lilima@cc.usu.edu, {yqchen, moorek}@ece.usu.edu

***Abstract*— This paper presents linear approximation ideas to range identification problem for a perspective dynamic system (PDS). Using a recently introduced linear approximation technique, the perspective dynamic system, which is a special class of nonlinear systems, can be approximated by a sequence of linear, time-varying (LTV) subsystems. Observer design problem of the original nonlinear PDS reduces to the observer design of this sequence of LTV subsystems. For each LTV subsystem, existing standard observer methods can be applied.**

I. Introduction

Recently, vision systems have been used broadly in a variety of applications, such as robot navigation, assembly line operation, and automatic video surveillance, due to its easy acquiring of data and the rich information in the data. Within these vision applications, it is always desirable to estimate motion dynamics of a moving object from image sequences, such as obstacle avoidance for robots and visual feedback for assembly line operations. Among various 3-D motion estimation algorithms, algorithms that arise from control point of view has been established in perspective dynamic system (PDS) framework. The PDS is a special class of nonlinear systems with linear dynamic system and homogeneous observation functions.

With a stationary camera observing a moving object, we assume that the object follows an affine motion described by

$$\begin{bmatrix} \dot{X}(t) \\ \dot{Y}(t) \\ \dot{Z}(t) \end{bmatrix} = \begin{bmatrix} a_{11} & a_{12} & a_{13} \\ a_{21} & a_{22} & a_{23} \\ a_{31} & a_{32} & a_{33} \end{bmatrix} \begin{bmatrix} X(t) \\ Y(t) \\ Z(t) \end{bmatrix} + \begin{bmatrix} b_1 \\ b_2 \\ b_3 \end{bmatrix}. \quad (1)$$

Then, a typical PDS will consist of the above linear dynamic system with the following homogeneous output observations:

$$y_1(t) = \frac{X(t)}{Z(t)}, \quad y_2(t) = \frac{Y(t)}{Z(t)}. \quad (2)$$

Basic issues relating to a PDS include observability, identifiability, controllability problems [1], [2], [3], [4], and range identification task [4], [5], [6] etc. This paper concerns the range identification for a PDS using linear approximation based nonlinear observers. The range identification problem can be formally defined as: assuming that the motion parameters $a_{i,j}$ and b_i in (1) for $i, j = 1, 2, 3$ are known, to estimate the position of an object with an unknown initial condition from observations on the imaging surface [4], [5], [6].

Range identification for a PDS via nonlinear observers has been proposed since 1990's. Typical nonlinear observers applied to the range identification problem, referred to as perspective nonlinear observers hereafter, include the identifier based observer (IBO) presented in [4], the state observer (referred to as SMO due to the employment of sliding mode method) in [5], and the range identification observer (RIO) in [6].

For a general nonlinear system, observer design techniques fall into the following categories:

1) Assuming bounded or local/global Lipschitz conditions.
2) Lyapunov based design.
3) Linear approximation based technique.
4) Via transformations [7].

The IBO and SMO observers belong to the first category, while the RIO belongs to the second. In this paper, perspective nonlinear observer design is pursued in the linear approximation category, where the nonlinear system is approximated by a sequence of LTV subsystems. Observer design of the original nonlinear system reduces to the observer design of this sequence of LTV subsystems, allowing the use of well-known linear techniques [8], [9].

The paper is organized as follows. Section II introduces the linear approximation technique and applies this technique to the range identification problem. For each approximation subsystem of the original PDS, observer design is carried out using the LTV observer in [10], whose detailed procedures are presented in Sec. III. Section IV presents simulation results of the linear approximation based observer with comparisons among several other perspective nonlinear observers for the range identification problem. Finally, section V concludes the paper.

II. Linear Approximation Technique

A. Introduction to Linear Approximation Technique

A recently developed method for replacing a nonlinear system by a sequence of LTV approximations is briefly described,

† Corresponding author. Tel. (435)797-0148, Fax: (435)797-3054. CSOIS URL: http://www.csois.usu.edu/

where the sequence of LTV subsystems converges on any compact time interval, uniformly in time, to the solution of the original nonlinear system under the condition of local Lipschitz. Consider the following nonlinear system

$$\begin{aligned} \dot{x}(t) &= A(x)x(t) + B(x)u(t), \\ y(t) &= C(x)x(t), \end{aligned} \tag{3}$$

with $x(0) = x_0 \in \mathbb{R}^n$. The sequence of LTV approximations is introduced as [8], [9]:

$$\begin{cases} \dot{x}^{[0]}(t) = A(x_0)x^{[0]}(t) + B(x_0)u^{[0]}(t), \\ \dot{x}^{[i]}(t) = A(x^{[i-1]}(t))x^{[i]}(t) + B(x^{[i-1]}(t))u^{[i]}(t), \\ x^{[0]}(t) = x_0, \text{ for } i = 0, \quad x^{[i]}(t) = x_0, \text{ for } i \geq 1. \end{cases} \tag{4}$$

Using the above linear approximations, global convergence is guaranteed in the sense that if the solution of the original nonlinear system exists and is bounded in the interval $[0, \tau] \subseteq \mathbb{R}$, then the sequence of LTV approximations converges uniformly on $[0, \tau]$ to the solution of the original nonlinear system [9].

B. Linearization of PDS

Define $y_3(t) = 1/Z(t)$. The range identification problem discussed is to estimate $Z(t)$, or its inverse $y_3(t)$. Let $y(t) = [y_1(t), y_2(t), y_3(t)]^T$. The derivative of $y(t)$ is:

$$\begin{cases} \dot{y}_1(t) = a_{13} + (a_{11} - a_{33})y_1 + a_{12}y_2 - a_{31}y_1^2 \\ \qquad\qquad - a_{32}y_1y_2 + (b_1 - b_3y_1)y_3, \\ \dot{y}_2(t) = a_{23} + a_{21}y_1 + (a_{22} - a_{33})y_2 - a_{31}y_1y_2 \\ \qquad\qquad - a_{32}y_2^2 + (b_2 - b_3y_2)y_3, \\ \dot{y}_3(t) = -(a_{31}y_1 + a_{32}y_2 + a_{33})y_3 - b_3y_3^2. \end{cases} \tag{5}$$

From now on, we use the vector variable x to denote the state vector in (5) to be consistent with the general nonlinear system (3).

After changing the variables, the dynamics (5) can be rewritten in the form of (3) as:

$$\begin{aligned} \dot{x}(t) &= \underbrace{\begin{bmatrix} a_{11} - Q_1(t) & a_{12} & b_1 - b_3x_1 \\ a_{21} & a_{22} - Q_1(t) & b_2 - b_3x_2 \\ 0 & 0 & -Q_1(t) - b_3x_3 \end{bmatrix}}_{A(x)} x(t) \\ &\quad + \underbrace{\begin{bmatrix} a_{13} & a_{23} & 0 \end{bmatrix}^T}_{B^T(x)}, \\ y(t) &= \underbrace{\begin{bmatrix} 1 & 0 & 0 \\ 0 & 1 & 0 \end{bmatrix}}_{C(x)} x(t), \quad x(0) = x_0, \end{aligned} \tag{6}$$

with

$$Q_1(t) = a_{33} + a_{31}x_1 + a_{32}x_2. \tag{7}$$

Applying the linear approximation idea described in Sec. II-A, the nonlinear system (6) can be replaced by a sequence of linear approximations specifically of the form:

$$\begin{aligned} &\dot{x}^{[i]}(t) = \\ &\underbrace{\begin{bmatrix} a_{11} - Q_1^{[i-1]} & a_{12} & b_1 - b_3x_1^{[i-1]} \\ a_{21} & a_{22} - Q_1^{[i-1]} & b_2 - b_3x_2^{[i-1]} \\ 0 & 0 & -Q_1^{[i-1]} - b_3x_3^{[i-1]} \end{bmatrix}}_{A(x^{[i-1]}(t))} x^{[i]}(t) \\ &+ \underbrace{\begin{bmatrix} a_{13} & a_{23} & 0 \end{bmatrix}^T}_{B^T(t)}, \\ &y^{[i]}(t) = \underbrace{\begin{bmatrix} 1 & 0 & 0 \\ 0 & 1 & 0 \end{bmatrix}}_{C(t)} x^{[i]}(t), \quad x^{[i]}(0) = x_0, \end{aligned} \tag{8}$$

where $x^{[-1]}(t) = x_0$ for $i = 0$, $Q_1^{[i]}(t) = a_{33} + a_{31}x_1^{[i]} + a_{32}x_2^{[i]}$, and $B(t)$ and $C(t)$ are constant matrices.

III. Observer Design for LTV Systems

Using the sequence of LTV approximations in (4), the observer design of the original nonlinear system can be converted to the observer design of this sequence of LTV subsystems. In [8], the state estimation of each LTV subsystem is performed using the algorithm in [10] due to its simplicity in implementation. For the range identification problem in concern, the LTV observer in [10] is temporarily adopted to illustrate the idea in this paper. Other LTV observer techniques can also be applied.

A. LTV Observer for Each Approximation Subsystem

Consider (8) and assume temporarily that $x^{[i-1]}(t)$ and $y^{[i]}(t)$ are known signals for the i-th approximation subsystem. Each approximation subsystem can be regarded as a stand alone LTV system in the form

$$\begin{aligned} \dot{x}(t) &= A(t)x(t) + B(t)u(t), \\ y(t) &= C(t)x(t), \end{aligned} \tag{9}$$

where $A(t) = A(x^{[i-1]}(t))$ is available since $x^{[i-1]}(t)$ is assumed known. $B(t)$ and $C(t)$ are constant matrices and $u(t) = 1$. Based on these assumptions, the following sequence of LTV observers can be constructed as in [8] using the observer design algorithm of [10] for the sequence of LTV subsystems:

$$\begin{cases} \dot{\hat{\bar{x}}}^{[0]}(t) = \bar{F}\hat{\bar{x}}^{[0]}(t) + \bar{G}(x_0)y^{[0]}(t) + \bar{B}(x_0)u^{[0]}(t), \\ \dot{\hat{\bar{x}}}^{[i]}(t) = \bar{F}\hat{\bar{x}}^{[i]}(t) + \bar{G}(x^{[i-1]})y^{[i]}(t) + \bar{B}(x^{[i-1]})u^{[i]}(t), \\ x^{[0]}(0) = x_0, \text{ for } i = 0, \quad x^{[i]}(0) = x_0, \text{ for } i \geq 1, \end{cases} \tag{10}$$

with

$$\hat{x}^{[i]}(t) = P(t)\,\hat{\bar{x}}^{[i]}(t), \quad \text{for } i \geq 0, \tag{11}$$

where $P(t)$ is a Lyapunov transformation to be designed. The matrices $\bar{B}$, $\bar{G}$, and $\bar{F}$ can be calibrated from $P(t)$ as to be shown in equations (17), (20), and (22).

In the following, detailed LTV observer design procedures in [10] are given for each LTV subsystem of a PDS. The readers are strongly recommended to refer [10] for notations and algorithms.

Using the same variables as in [10], for the i-th subsystem, the observability matrix is

$$N(t) = [N_1(t), N_2(t)]^T, \tag{12}$$

where

$$N_1(t) = C(t) = \begin{bmatrix} 1 & 0 & 0 \\ 0 & 1 & 0 \end{bmatrix},$$
$$\begin{aligned} N_2(t) &= C(t)A(t) \\ &= \begin{bmatrix} a_{11} - Q_1^{[i-1]} & a_{12} & b_1 - b_3 x_1^{[i-1]} \\ a_{21} & a_{22} - Q_1^{[i-1]} & b_2 - b_3 x_2^{[i-1]} \end{bmatrix}. \end{aligned} \tag{13}$$

If $N(t)$ is of full rank and if one row of $N_2(t)$, say the first row, is always linearly independent with the two rows of $N_1(t)$ for all $t \in [0, \infty]$, we can form a matrix $\bar{N}(t)$

$$\bar{N}(t) = \begin{bmatrix} 1 & 0 & 0 \\ a_{11} - Q_1^{[i-1]}(t) & a_{12} & b_1 - b_3 x_1^{[i-1]} \\ 0 & 1 & 0 \end{bmatrix}, \tag{14}$$

whose inverse exists with the following form:

$$\bar{N}^{-1}(t) = \begin{bmatrix} 1 & 0 & 0 \\ 0 & 0 & 1 \\ \frac{Q_1^{[i-1]}(t) - a_{11}}{b_1 - b_3 x_1^{[i-1]}} & \frac{1}{b_1 - b_3 x_1^{[i-1]}} & \frac{-a_{12}}{b_1 - b_3 x_1^{[i-1]}} \end{bmatrix}. \tag{15}$$

It has been noticed that the observability indices are $n_1 = 2$ and $n_2 = 1$. A Lyapunov transformation $P(t)$ can be constructed as

$$P(t) = [A(t)\alpha_1 - \dot{\alpha}_1, \quad \alpha_1, \quad \alpha_2], \tag{16}$$

where α_1 and α_2 are the 2-nd and the 3-rd column of $\bar{N}^{-1}(t)$, respectively.

After getting $P(t)$ and following the algorithm procedures in [10], we have:

1) Obtain $\bar{A}(t), \bar{B}(t), \bar{C}(t)$:

$$\begin{aligned} \bar{A}(t) &= P^{-1}(t)\,(A(t)P(t) - \dot{P}(t)), \\ \bar{B}(t) &= P^{-1}(t)\,B(t) = P^{-1}(t)[a_{13},\, a_{23},\, 0]^T, \\ \bar{C}(t) &= C(t)\,P(t). \end{aligned} \tag{17}$$

From (17), the calculation of $\bar{A}(t)$ requires the calculation of $\dot{P}(t)$. If $\bar{N}(t)$ is a constant matrix, α_1 and α_2 are constant vectors. Then, $P(t)$ becomes $[A(t)\,\alpha_1, \alpha_1, \alpha_2]$, which contains at most $x^{[i-1]}(t)$. In this case, the calculation of $\dot{P}(t)$ only requires $\dot{x}^{[i-1]}(t)$ besides $x^{[i-1]}(t)$. However, if α_1 is not constant, but having terms of $x^{[i-1]}(t)$, we are in a more complex situation to calculate $\ddot{x}^{[i-1]}(t)$. Notice that in the linear approximation framework, the input signal $x^{[i-1]}(t)$ to the i-th subsystem has no analytical formula, which is different from the situation when $A(t), B(t), C(t)$ in (9) has analytical formulae of t, where the matrix $P(t)$ is also in an analytical form and its derivative $\dot{P}(t)$ can be calculated straightforward.

To calculate $\ddot{x}^{[i-1]}(t)$, more information is needed besides $\dot{x}^{[i-1]}(t)$ and $x^{[i-1]}(t)$. This is because:

$$\begin{aligned} \ddot{x}^{[i-1]}(t) &= \frac{d}{dt}[\dot{x}^{[i-1]}(t)], \\ &= \frac{d}{dt}\left[A(x^{[i-2]})x^{[i-1]}(t) + \begin{bmatrix} a_{13} \\ a_{23} \\ 0 \end{bmatrix}\right], \\ &= A(x^{[i-2]})\dot{x}^{[i-1]}(t) + \dot{A}(x^{[i-2]})x^{[i-1]}(t). \end{aligned} \tag{18}$$

In the above equation, the calculation of $\dot{A}(x^{[i-2]})$ requires $\dot{x}^{[i-2]}(t)$. Thus, the input to each LTV subsystem for the range identification problem include $x^{[i-2]}(t)$ and $\dot{x}^{[i-2]}(t)$, as well as $x^{[i-1]}(t)$ and $\dot{x}^{[i-1]}(t)$.

2) Choose the desired eigenvalues $(\lambda_1, \lambda_2, \lambda_3)$. The resulting coefficients of the characteristic polynomial are $(\beta_0, \beta_1, \beta_2)$ in the form of

$$\prod_{i=1}^{n}(\lambda - \lambda_i) = \lambda^n + \beta_{n-1}\lambda^{n-1} + \cdots + \beta_1\lambda + \beta_0. \tag{19}$$

3) Obtain $\bar{G}(t)$:

$$\bar{G}(t) = (A_2 - A_3 + A_4)C_1^{-1}, \tag{20}$$

where

$$\begin{aligned} &A_2 = [\bar{A}(:,1),\, \bar{A}(:,3)], \quad C_1 = [\bar{C}(:,1),\, \bar{C}(:,3)], \\ &A_3 = \begin{bmatrix} 0 & 0 \\ 0 & 1 \\ 0 & 0 \end{bmatrix}, \quad A_4 = \begin{bmatrix} \beta_0 & 0 \\ \beta_1 & 0 \\ \beta_2 & 0 \end{bmatrix}, \end{aligned} \tag{21}$$

and where $\bar{A}(:,i)$ and $\bar{C}(:,j)$ denote the i-th and the j-th column of $\bar{A}$ and $\bar{C}$, respectively.

4) $\bar{F}(t)$: Using the above design procedures, $\bar{F}(t)$ becomes

$$\bar{F}(t) = \begin{bmatrix} -\beta_0 & 1 & 0 \\ -\beta_1 & 0 & 1 \\ -\beta_2 & 0 & 0 \end{bmatrix}. \tag{22}$$

B. *Comments on Availability of Signals*

In the LTV observer (10), it is assumed that $x_0, x^{[i-1]}(t)$ and $y^{[i]}(t)$ are known signals for the i-th approximation subsystem. Unfortunately, the signals $x_0, x^{[i-1]}(t)$ and $y^{[i]}(t)$ are unknown from the original nonlinear system (6). If $x_0, A(x), B(x)$ are all assumed known, all the information of the original nonlinear system is available and there is no need to construct an observer. In other words, the fundamental nature of an observer is messed up using the "observer" in (10).

Then, how the linear approximation technique can help for the observer design of an original nonlinear system? For the PDS in (6), $C(x)$ is a constant matrix. Outputs of the sequence of LTV subsystems will converge to the actual output $y(t)$ of the original nonlinear system. That is:

$$\lim_{t\to\infty} y^{[i]}(t) = y(t), \quad \text{as } i \to \infty. \tag{23}$$

By replacing $y^{[i]}(t)$ with $y(t)$ and $x^{[i-1]}(t)$ with $\hat{x}^{[i-1]}(t)$, we construct the following sequence of LTV observers, which we call LAO for an abbreviation of linear approximation observer:

$$\text{LAO}\begin{cases} \dot{\hat{\bar{x}}}^{[0]}(t) = \bar{F}\,\hat{\bar{x}}^{[0]}(t) + \bar{G}(x_0')\,y(t) + \bar{B}\,u(t), \\ \dot{\hat{\bar{x}}}^{[i]}(t) = \bar{F}\,\hat{\bar{x}}^{[i]}(t) + \bar{G}(\hat{x}^{[i-1]})\,y(t) + \bar{B}\,u(t), \\ x^{[0]}(0) = x_0',\ \text{for } i = 0, \quad x^{[i]}(0) = x_0',\ \text{for } i \geq 1, \end{cases} \tag{24}$$

with

$$\hat{x}^{[i]}(t) = P(t)\,\hat{\bar{x}}^{[i]}(t), \quad \text{for } i \geq 0,$$

where $u(t)$ and $y(t)$ are the input and output of the original nonlinear system (6). $\hat{x}^{[i-1]}(t)$ is the state estimation from the (i-1)-th subsystem.

In (24), the state estimate is denoted by $\hat{x}^{[i]}(t)$ as an abuse of the variable. It is worthy emphasizing that $\hat{x}^{[i]}(t)$ is not the estimate of $x^{[i]}(t)$, but the estimate of state $x(t)$ of the original nonlinear system. Besides, the initial conditions of each LTV subsystem are chosen to be x_0', which is different from x_0. As noticed, based on the linear approximation techniques, a sequence of observers needs to be constructed. Fortunately, this drawback is not that severe due to the modularity feature of each observer.

The application of the LTV observer in [10] requires the LTV system to be uniformly observable ($N(t)$ is invertible) and have a lexicographic basis (one row in $N_2(t)$ in (13) must always be able to form a 3×3 nonsingular matrix with $N_1(t)$). Obviously, the above observability condition of the LTV observer imposes restrictions on the overall LAO observer. LTV observers that have less restricted observability conditions, possibly with only mild Lipschitz requirement, thus need to be investigated and applied. Due to the above mentioned restriction, the LTV observer in [10] is only temporarily applied to illustrate the main point of this work. That is, after applying the linear approximation technique, observer design of a nonlinear system can be reduced to the conventional observer design of a sequence of LTV systems.

Remark 3.1: The linear approximation based observer can be applicable to general nonlinear systems that satisfy the mild local Lipschitz condition for linear approximation, not just a special class of nonlinear systems, as for which the IBO, SMO, and RIO are designed. Further, for a PDS with possible more general nonlinear imaging surface, this LAO can still be applied.

IV. Simulation Results and Discussions

Simulation results of the LAO observer are presented along with three other perspective nonlinear observers, the IBO [4], SMO [5], and RIO [6], for a PDS system when the target is moving according to the following affine motions:

1) $\mathbf{Motion_1}$:

$$\begin{bmatrix} \dot{X} \\ \dot{Y} \\ \dot{Z} \end{bmatrix} = \begin{bmatrix} -0.2301 & 0.4043 & -0.5769 \\ 0.1276 & -0.3003 & 0.2839 \\ 0.2450 & -0.4247 & 0.4319 \end{bmatrix} \begin{bmatrix} X \\ Y \\ Z \end{bmatrix} + \begin{bmatrix} 0.5 \\ 0.25 \\ 0.3 \end{bmatrix}, \quad [X_0, Y_0, Z_0]^T = [0.4, 0.6, 1.0]^T. \tag{25}$$

2) $\mathbf{Motion_2}$:

$$\begin{bmatrix} \dot{X} \\ \dot{Y} \\ \dot{Z} \end{bmatrix} = \begin{bmatrix} -1.7073 & -0.6368 & -1.0540 \\ 0.2279 & -1.0026 & -0.0715 \\ 0.6856 & -0.1856 & 0.2792 \end{bmatrix} \begin{bmatrix} X \\ Y \\ Z \end{bmatrix} + \begin{bmatrix} 0.5 \\ 0.25 \\ 0.3 \end{bmatrix}, \quad [X_0, Y_0, Z_0]^T = [0.4, 0.6, 1.0]^T. \tag{26}$$

In this section, the linear approximation technique is first implemented to verify/show, via example, how the $x^{[i]}(t)$ signals in (4) converge to the state $x(t)$ of the nonlinear system. Secondly, detailed experimental results are presented for the LAO observer's convergence using the two motions in (25) and (26), where we again emphasize that the state estimates $\hat{x}^{[i]}(t)$ in (24) converge to the actual state $x(t)$ of the nonlinear system, not the $x^{[i]}(t)$ in (4). Finally, performance comparisons of our LAO with the other three perspective nonlinear observers are presented.

A. Simulation Validation of Linear Approximation Technique

Given a nonlinear system (3), if all the information about the system is known, i.e., its initial condition, its structure, its parameters, and its input, then a sequence of LTV subsystems can be formed, as illustrated in Fig. 1. In each subsystem of the sequence, it receives $x^{[i-1]}(t)$ signal from its previous block such that the matrices $A(x^{[i-1]}(t)), B(x^{[i-1]}(t)), C(x^{[i-1]}(t))$ can be determined. In this way, each subsystem becomes a LTV system.

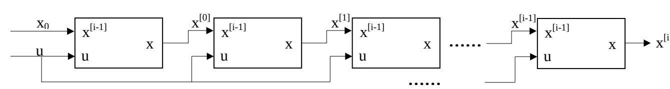

Fig. 1. A sequence of LTV subsystems of a nonlinear system.

Using $\mathbf{Motion_1}$, the states $x^{[i]}(t)$ for $i = 1, 2, 3$ are shown in Fig. 2. It is observed that the convergence pattern of $x^{[i]}(t)$ to $x(t)$ is up and down around $x(t)$, and finally converges to $x(t)$.

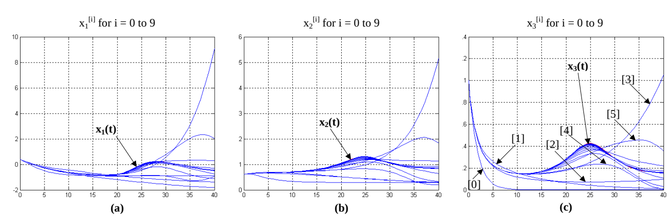

Fig. 2. $x^{[i]}_{1,2,3}(t)$ of (8) under $\mathbf{Motion_1}$ without noise.

B. Performance Study of LAO Observer

Block diagram of the LAO observer is shown in Fig. 3, where the inputs to each observer module include: 1) the actual output of the original nonlinear system, 2) the control input, and 3) $P(t), \bar{F}(t), \bar{B}(t), \bar{G}(t)$ calculated using $\hat{x}^{[i-1]}(t)$, $\dot{\hat{x}}^{[i-1]}(t)$ and possibly $\hat{x}^{[i-2]}(t)$, $\dot{\hat{x}}^{[i-2]}(t)$ signals. The "LTVObs" function, implemented by a S-function in

Matlab Simulink due to its demanding matrix manipulations, calculates the $P(t), \bar{F}(t), \bar{B}(t), \bar{G}(t)$ matrices in equations (16), (17), (20), and (22). With the above calculated matrices, the other part of the LTV observer module outputs the state estimates according to (11).

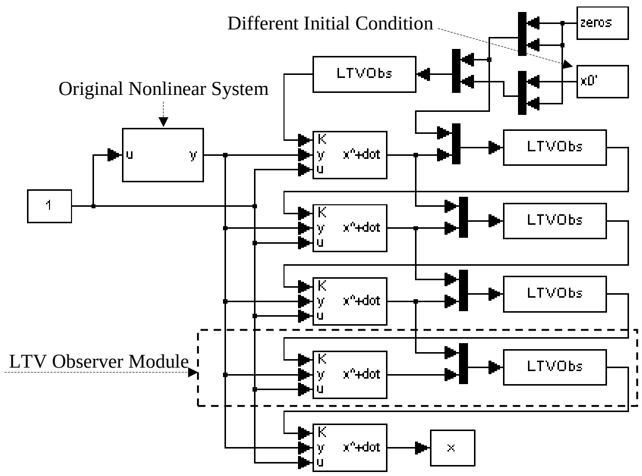

Fig. 3. Matlab simulation block diagram of the LAO observer.

Under $\mathbf{Motion_1}$ and $\mathbf{Motion_2}$, the LAO observer is tested in the cases of no noise and with uniform noise bounded by $\pm 10^{-2}$ with two different initial conditions $x_0' = [0, 0, 0]^T$ and $x_0' = [-1, 2, 1]^T$. In this paper, only simulation results with $x_0' = [0, 0, 0]^T$ are presented to save space and maintain clarity. The design parameters for the LAO observer are $\lambda_1 = -1,\ \lambda_2 = -2,\ \lambda_3 = -3$. That is, $\beta_0 = 6,\ \beta_1 = 11,\ \beta_2 = 6$.

In Fig. 4, $\hat{x}_{1,2,3}^{[i]}(t)$ for $i = 0, \ldots, 9$ are plotted together with their true state trajectories for the ideal case of no noise. To extensively test the LAO observer, the simulation time is set to be 80 seconds. It is observed that as i increases, $\hat{x}_{1,2,3}^{[i]}(t)$ reach $x_{1,2,3}(t)$ closer and closer. The LAO is also tested when the output is corrupted with uniform noise bounded by $\pm 10^{-2}$, as shown in Fig. 5. Compared with Fig. 4, $\hat{x}_{1,2,3}^{[i]}(t)$ in Fig. 5 are more noisy, but still showing good convergence to their true trajectories.

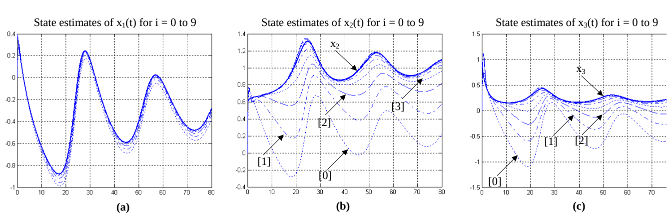

Fig. 4. $\hat{x}_{1,2,3}^{[i]}(t)$ under $\mathbf{Motion_1}$ without noise.

The above simulations are also performed using $\mathbf{Motion_2}$, where the corresponding results are shown in Figs. 6 and 7, respectively. The simulation time is set to be 20 seconds due to the simple varying pattern of the system's outputs.

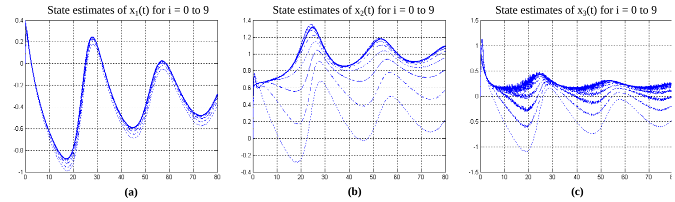

Fig. 5. $\hat{x}_{1,2,3}^{[i]}(t)$ under $\mathbf{Motion_1}$ with uniform noise bounded by $\pm 10^{-2}$.

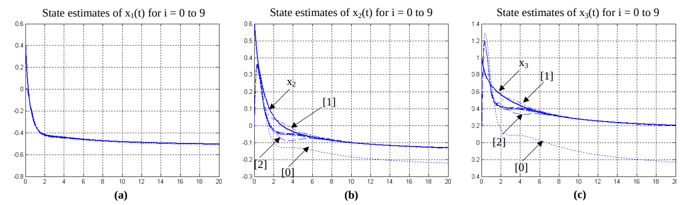

Fig. 6. $\hat{x}_{1,2,3}^{[i]}(t)$ under $\mathbf{Motion_2}$ without noise.

C. Comparison Among Perspective Nonlinear Observers

At the last part of simulations, a comparison between the LAO and the other three perspective nonlinear observers is performed using the two motions in (25) and (26), where the simulation results are shown in Figs. 8 and 9, respectively. In these comparisons, we use $x_0' = [0, 0, 0]^T$. The observer parameters for the other three observers are listed in the following using the same variables as in the corresponding original papers [4], [5], [6]:

1) IBO: $M = 10, G = 10, \gamma = 1, A = I_{2\times 2}, P = -I_{2\times 2}/2$, where $I_{2\times 2}$ denotes the identity matrix of dimension 2.
2) SMO: $M = 10, \alpha = 5, \alpha_1 = \alpha_2 = 10, \delta_1 = \delta_2 = 0.2, \hat{\lambda}_1(0) = \hat{\lambda}_2(0) = 1$.
3) RIO: $\gamma_1 = \gamma_2 = 30, k_{s1} = k_{s2} = 5, \alpha_1 = \alpha_2 = 5$.

The above observer parameters are selected based on a similar converging speed in the absence of noise along with acceptable performance in the presence of noise.

Figures 8 and 9 show the state estimation error, $x_3(t) - \hat{x}_3(t)$, for all the four observers. Note that in Figs. 8 and 9, $\hat{x}_3^{[9]}(t)$ is taken as $\hat{x}(t)$ for the LAO observer. In Fig. 8, the plots in (a) and (b) are the comparisons among the four observers in the ideal case of no noise, while (c) and (d) show the comparison in the presence of uniform noise bounded by $\pm 10^{-2}$. Similarly, in Fig. 9, (a) shows the results without noise and (b) with uniform noise. Notice that a different simulation time (80 seconds) is used in Fig. 8 for the LAO for an

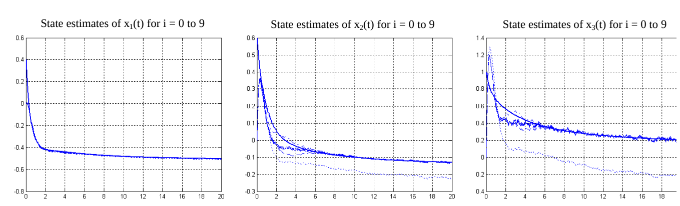

Fig. 7. $\hat{x}_{1,2,3}^{[i]}(t)$ under $\mathbf{Motion_2}$ with uniform noise bounded by $\pm 10^{-2}$.

extensive testing of its performance. From Figs. 8 and 9, it can be observed that the LAO observer has a slower converging speed than the other three observers designed specifically for the PDS. Though different observer design parameters might result in different converging speed, it is not surprising that the LAO, which is based on the linear approximation technique applicable to more general nonlinear systems, would not perform as well as the perspective nonlinear observers designed specifically for a PDS, as the other three observers in comparison.

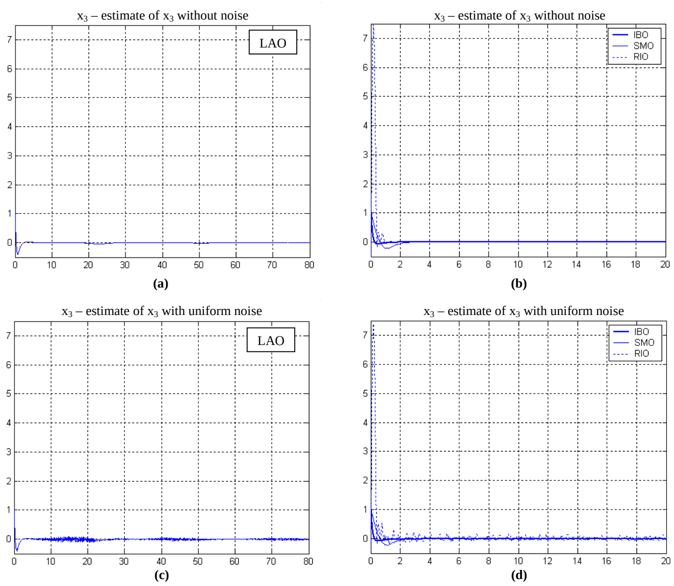

Fig. 8. Comparison of LAO with the other three perspective nonlinear observers under $\mathbf{Motion_1}$ with $x_0 = [0.4, 0.6, 1.0]^T$ and $x'_0 = [0, 0, 0]^T$: (a, b) without noise; (c, d) with uniform noise bounded by $\pm 10^{-2}$.

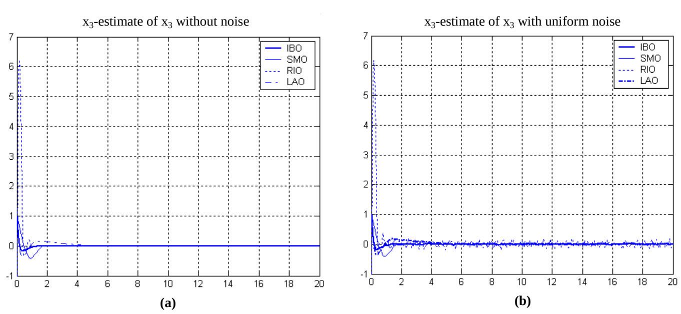

Fig. 9. Comparison of LAO with the other three perspective nonlinear observers under $\mathbf{Motion_2}$ with $x_0 = [0.4, 0.6, 1.0]^T$ and $x'_0 = [0, 0, 0]^T$: (a, b) without noise; (c, d) with uniform noise bounded by $\pm 10^{-2}$.

V. Concluding Remarks

In this paper, a recently developed linear approximation technique, which replaces a general nonlinear system (satisfying local Lipschitz condition) by a sequence of linear time-varying (LTV) approximations, is used for the design of a state observer for the range identification of a perspective dynamic system (PDS). Using the linear approximation idea, state estimation of the original nonlinear system is reduced to a state estimation of a sequence of LTV subsystems, where standard linear methods can be applied. Since the linear approximation based observer is applicable to a broad class of nonlinear systems, when applied to the range identification problem, it has a slower converging speed compared to several other nonlinear observers designed specifically for a PDS. Moreover, observability condition of the LTV observer imposes a restriction on the resultant overall observer. LTV observers with less restricted condition thus need to be investigated and applied in this linear approximation framework. However, the LAO observer proposed in this paper has a straightforward application to PDS with more general setup, e.g. with a general imaging surface as in certain omnidirectional vision systems.

References

[1] B. K. Ghosh and E. P. Loucks, “A perspective theory for motion and shape estimation in machine vision,” *SIAM Journal of Control and Optimization*, vol. 35, no. 5, pp. 1530–1559, 1995.

[2] B. K. Ghosh, H. Inaba, and S. Takahashi, “Identification of Riccati dynamics under perspective and orthographic observations,” *IEEE Transactions on Automatic Control*, vol. 45, no. 7, pp. 1267–1278, July 2000.

[3] B. K. Ghosh and C. F. Martin, “Homogeneous dynamical systems theory,” *IEEE Transactions on Automatic Control*, vol. 47, no. 3, pp. 462–472, Mar. 2002.

[4] M. Jankovic and B. K. Ghosh, “Visually guided ranging from observations of points, lines and curves via an identifier based nonlinear observer,” *Systems and Control Letters*, vol. 25, pp. 63–73, 1995.

[5] X. Chen and H. Kano, “A new state observer for perspective systems,” *IEEE Transactions on Automatic Control*, vol. 47, no. 4, pp. 658–663, Apr. 2002.

[6] W. E. D. an Y. Fang, D. M. Dawson, and T. J. Flynn, “Range identification for perspective vision systems,” in *Proceedings of the American Control Conf.*, Denver, Colorado, U.S.A, June 4-6 2003, pp. 3448–3453.

[7] X. Xia and M. Zeitz, “On nonlinear continuous observers,” *Int. Journal of Control*, vol. 66, no. 6, pp. 943–954, 1997.

[8] C. N. Hernandez, S. P. Banks, and M. Aldeen, “Observer design for nonlinear systems using linear approximations,” *IMA Journal of Mathematical Control and Information*, vol. 20, pp. 359–370, 2003.

[9] M. Tomas-Rodriguez and S. P. Banks, “Linear approximations to nonlinear dynamical systems with applications to stability and spectral theory,” *IMA Journal of Mathematical Control and Information*, vol. 20, pp. 89–103, 2003.

[10] C. Nguyen and T. Lee, “Design of a state estimator for a class of time-varying multivariable systems,” *IEEE Transactions on Automatic Control*, vol. 30, no. 2, pp. 179–182, Feb. 1985.